arXiv:1303.4720v1 [cond-mat.soft] 19 Mar 2013

Defect annihilation and proliferation in active nematics

Luca Giomi,[1] M. J. Bowick,[2,3] Xu Ma,[2] and M. Cristina Marchetti[2,3]
[1] *SISSA, International School for Advanced Studies, Via Bonomea 265, 34136 Trieste, Italy*
[2] *Physics Department, Syracuse University, Syracuse NY 13244, USA*
[3] *Syracuse Biomaterials Institute, Syracuse University, Syracuse NY 13244, USA*

Liquid crystals inevitably possess topological defect excitations generated through boundary conditions, applied fields or in quenches to the ordered phase. In equilibrium pairs of defects coarsen and annihilate as the uniform ground state is approached. Here we show that defects in active liquid crystals exhibit profoundly different behavior, depending on the degree of activity and its contractile or extensile character. While contractile systems enhance the annihilation dynamics of passive systems, extensile systems act to drive defects apart so that they swarm around in the manner of topologically well-characterized self-propelled particles. We develop a simple analytical model for the defect dynamics which reproduces the key features of both the numerical solutions and recent experiments on microtuble-kinesin assemblies.

Active liquid crystals are nonequilibrium fluids composed of internally driven elongated units. The key feature that distinguishes them from their well-studied passive counterparts is that they are maintained out of equilibrium not by an external force applied at the system's boundary, such as an imposed shear, but by an energy input on each individual unit. Examples include mixtures of cytoskeletal filaments and associated motor proteins, bacterial suspensions, the cell cytoskeleton and even nonliving analogues, such as monolayers of vibrated granular rods [1]. The internal drive that characterizes active liquid crystals dramatically changes the systems dynamics and yields novel effects arising from the interplay of orientational order and flow, such as spontaneous laminar flow [2–4], large density fluctuations [5–7], unusual rheological properties [8–10], excitability [11, 12] and low Reynolds number turbulence [12, 13].

Ordered liquid crystalline phases of active matter, like their equilibrium counterparts, exhibit distinctive inhomogeneous configurations known as topological defects. In equilibrium, defect configurations may be generated through boundary conditions, externally applied fields, or via rapid quenches into the ordered state. When the constraints are removed or the system is given time to equilibrate, the defects ultimately annihilate [14]. Experiments have shown that in active systems, in contrast, defect configurations can occur spontaneously in bulk and be continuously regenerated by the local energy input [15, 16]. The nature of the topological defects is of course intimately related to the symmetry of the system, which can be either polar (like in ferromagnets) or nematic. While the nature of the charge +1 defects that occur in polar active systems has been studied for some time [17–20], the properties of defects in apolar or nematic active media is still largely unexplored. In these systems the defects are charge ±1/2 disclinations [21]. Such defects have been identified in monolayers of vibrated granular rods [7] and in active nematic gels assembled in vitro from microtubules and kinesins, where they were shown to control spontaneous flows in bulk [16]. Furthermore, when confined at a water/oil interface, the gel forms a two-dimensional active nematic film, with self-sustained flows resembling cytoplasmic streaming, and the continuous creation and annihilation of disclination defect pairs [16].

In this paper we examine the effect of activity on the dynamics of disclinations in nematic liquid crystals. It is well known that hydrodynamics plays an important role in controlling the dynamics of defects in liquid crystals. As the defect moves, the coupling between the orientational order parameter and the flow velocity of the fluid yields what is usually called the *backflow* which significantly modifies defect dynamics [22–24]. Here we show that active stresses dramatically affect the defect dynamics by altering the backflow in such a way as to slow down, speed up or even suppress pair annihilation, according to the extent of activity and the typical time scale of orientational relaxation of the nematic phase. Moreover, when the latter is very large compared to the time scale associated with activity, relaxation is overwhelmed entirely, leading to defect proliferation.

The hydrodynamic equations of active nematic liquid crystals can be obtained from that of passive nematics by the addition of nonequilibrium stresses and currents due to activity [1, 11, 12]. They are formulated in terms of a concentration c, a flow velocity $\boldsymbol{v}$ and the nematic tensor order parameter $Q_{ij} = S\left(n_i n_j - \frac{1}{2}\delta_{ij}\right)$, with $\boldsymbol{n}$ the director field. Considering for simplicity the case of an incompressible fluid of constant density ρ, where $\boldsymbol{\nabla}\cdot\boldsymbol{v} = 0$, the equations are given by:

$$\frac{Dc}{Dt} = \partial_i\left[D_{ij}\partial_j c + \alpha_1 c^2 \partial_j Q_{ij}\right] \;, \tag{1a}$$

$$\rho\frac{Dv_i}{Dt} = \eta\Delta v_i - \partial_i p + \partial_j \sigma_{ij} \;, \tag{1b}$$

$$\frac{DQ_{ij}}{Dt} = \lambda S u_{ij} + Q_{ik}\omega_{kj} - \omega_{ik}Q_{kj} + \gamma^{-1}H_{ij} \;, \tag{1c}$$

where $\frac{D}{Dt} = \partial_t + \boldsymbol{v}\cdot\nabla$ indicates the material derivative, $D_{ij} = D_0\delta_{ij} + D_1 Q_{ij}$ is the anisotropic diffusion tensor, η

the viscosity, p the pressure and λ the nematic alignment parameter. Here $u_{ij} = (\partial_i v_j + \partial_j v_i)/2$ and $\omega_{ij} = (\partial_i v_j - \partial_j v_i)/2$ are the symmetrized rate of strain tensor and the vorticity, respectively. The molecular field H_{ij} embodies the relaxational dynamics of the nematic phase and can be obtained from the variation of the Landau-De Gennes free energy [21], $H_{ij} = -\delta F/\delta Q_{ij}$, with:

$$F/K = \int dA \, \left[\tfrac{1}{4}(c - c^\star) \operatorname{tr} \boldsymbol{Q}^2 + \tfrac{1}{4}c(\operatorname{tr} \boldsymbol{Q})^2 + \tfrac{1}{2}|\nabla \boldsymbol{Q}|^2\right] \ , \tag{2}$$

where K is an elastic constant with dimension of energy, $\operatorname{tr} \boldsymbol{Q}^2 = S^2/2$ and $c^\star$ is the critical concentration for the isotropic-nematic transition, so that, at equilibrium, $S = \sqrt{1 - c^\star/c}$. Finally, the stress tensor $\sigma_{ij} = \sigma^{\rm r}_{ij} + \sigma^{\rm a}_{ij}$ is the sum of the elastic stress due to nematic elasticity, $\sigma^{\rm r}_{ij} = -\lambda S H_{ij} + Q_{ik}H_{kj} - H_{ik}Q_{kj}$, where for simplicity we have neglected the Eriksen stress, and an active contribution, $\sigma^{\rm a}_{ij} = \alpha_2 c^2 Q_{ij}$, that describes tensile/contractile stresses exerted by the active particles in the direction of the director field. In addition, activity yields a curvature-induced current $\boldsymbol{j}^{\rm a} = -\alpha_1 c^2 \nabla \cdot \boldsymbol{Q}$ in Eq. (11) that drive units particles from regions populated by fast moving particles to regions of slow moving particles. The c^2 dependence of active stress and current is appropriate for systems where activity arises from pair interactions among the filaments via crosslinking motor proteins. The sign of α_2 depends on whether the active particles generate tensile or contractile stresses, with $\alpha_2 > 0$ for the contractile case and $\alpha_2 < 0$ for extensile systems, while $\alpha_1 > 0$. Below for simplicity we let $\alpha_2 = \alpha$ and take $\alpha_1 = |\alpha_2|/2$.

To study the dynamics of defects, we consider a pair of opposite-sign half-integer disclinations separated by a distance $x = x_+ - x_-$, where $x_\pm$ is the x-coordinate of the $\pm 1/2$ disclination as shown in Fig. 1a,b. When backflow is neglected, the pair dynamics is purely relaxational and is controlled by the balance of the attractive force between defects $\boldsymbol{F}_{\rm pair} = -\nabla E_{\rm pair}$, with $E_{\rm pair} \sim K \log x/a$ the energy of a defect pair (a the core radius), and an effective frictional force $\boldsymbol{F}_{\rm fric} = \mu \dot{\boldsymbol{x}}$, with $\mu \sim \gamma$ a friction coefficient. Thus $\mu \dot{x} = K/x$ and the distance between the annihilating defects decreases according to a square-root law, $x(t) \propto \sqrt{t_{\rm a} - t}$, with $t_{\rm a}$ the annihilation time. More precise calculations have shown that the effective friction is itself a function of the defect separation [25, 26], $\mu = \mu_0 \log x/a$, although this does not imply substantial changes in the overall picture. This simple model predicts that the two defects approach each other along symmetric trajectories.

We have integrated numerically Eqs. (1) for an initial configuration of uniform concentration and zero flow velocity, with two disclinations of charge $\pm 1/2$ located on the x axis of a square $L \times L$ box at initial positions $\boldsymbol{x}_\pm(0) = (\pm L/4, 0)$. To render Eqs. (1) dimensionless we normalize distance by the approximate length of the active rods $\ell = 1/\sqrt{c^\star}$, stress by the elastic stress of the nematic phase $\sigma = K\ell^{-2}$ and time by $\tau = \eta\ell^2/K$ representing the ratio between viscous and elastic stress. Periodic boundary conditions are assumed and the defects are allowed to evolve until they annihilate. Fig. 1 shows a snapshot of the order parameter and flow field shortly after the beginning of the relaxation for a contractile and tensile system, with $\alpha = \pm 0.2$ in the units defined above.

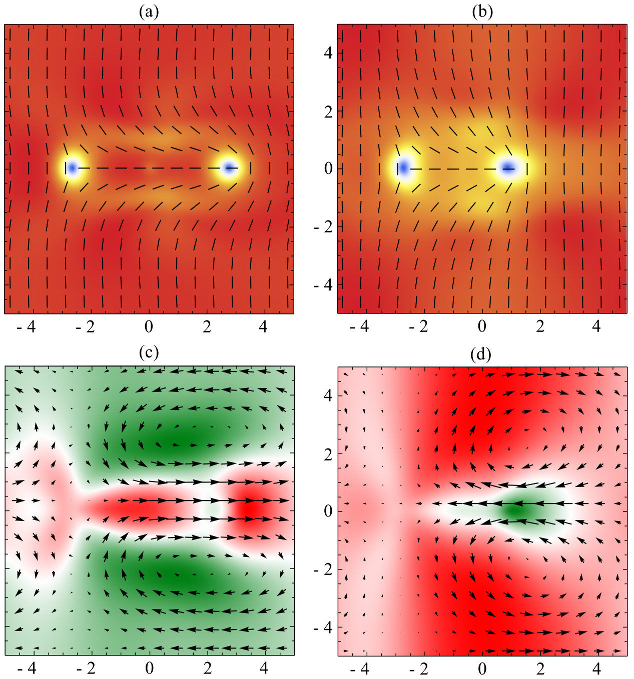

FIG. 1: Snapshots of a disclination pair shortly after the beginning of relaxation. (Top) Director field superimposed to a heat map of the nematic order parameter and (bottom) flow field superimposed to a heat map of the concentration for an extensile system with $\alpha = -0.2$ (a,c) and a contractile system with $\alpha = 0.2$ (b,d). According to the sign of α, the backflow tends to speed up ($\alpha > 0$) or slow down the ($\alpha < 0$) annihilation process by increasing/decreasing the velocity of the $+1/2$ disinclination. For α negative and sufficiently large in magnitude, the $+1/2$ defect reverses its direction of motion (a) and escapes from annihilation.

In passive nematic liquid crystals (i.e. $\alpha = 0$) the backflow has opposite effects on the dynamics of the $+1/2$ and the $-1/2$ defects. In the absence of backflow, the two defects move at the same velocity towards each other until annihilation, while backflow tends to speed up the $+1/2$ defect and to slow down the $-1/2$ defect [23]. Activity enters defect dynamics in two ways: via the curvature-driven active current proportional to α_1 and via the active stress proportional to α_2. It was noted before in the analysis of defect dynamics in vibrated monolayers of granular rods that curvature currents drive $+1/2$ defects to move in the direction of their "head", where the terminology arises from the comet-like shape of $+1/2$ defects, with a head and a tail [7]. In contrast the $-1/2$ defects remain stationary under the action of curvature currents. Backflow arising from director gradients in the stress tensor has the opposite effect and drives the $+1/2$ defect to move in the direction of its tail. This effect is greatly enhanced by activity for $\alpha > 0$, i.e, in contractile systems, and dominates over the curvature-current driven dynamics, yielding a net speed up of the $+1/2$ defects towards its opposite charge counterpart. The sign of the activity-induced backflow depends, however, on the sign of α. In extensile systems, with $\alpha < 0$ backflow drives the $+1/2$ defect to move towards its head, away from its $-1/2$ partner in the configuration of Fig. 1d, acting like an *effective repulsive interaction*. This interesting, and to some extent counterintuitive, effect has been observed in experiments with extensile microtubules and kinesin assemblies [16] and can be understood on the basis of the hydrodynamic approach embodied in Eqs. (1). In Fig. 2 we have reproduced from Ref. [16] a sequence of snapshots showing a pair of $\pm 1/2$ disclinations moving apart from each other together with the same behavior observed in our simulations.

To quantify the dynamics, we have reconstructed the trajectories of the defects by tracking the drop in the magnitude of the order parameter. The trajectories are shown in Fig. 3a,b where red lines in the upper portion of the plots represents the trajectory of the $+1/2$ disclination, while the blue lines in the lower portion of the plot are the trajectories of the $-1/2$ defect. The tracks interrupt when the cores of the two defect merge. For small activity and small values of the rotational friction γ, the trajectories resemble those obtained in Ref. [23] for passive systems. At large values of activity, however, the asymmetry in defect dynamics becomes more pronounced and when the activity dominates over orientational relaxation, the $+1/2$ disclination moves autonomously along its symmetry axis with a velocity $\boldsymbol{v} \propto \alpha\,\hat{\boldsymbol{x}}$, whose direction is dictated by the sign of α. This behavior is clearly visible in Fig. 3c showing the defect separation $x(t)$ as a function of time. For γ sufficiently large, the trajectories are characterized by two regimes. For large separations, the dynamics is dominated by the active backflow, thus $\dot{x}(t) \propto -\alpha$ and $x(t) \propto -\alpha t$. Once the defects are about to annihilate the attractive force $F_{\rm pair} \propto 1/x$ takes over and the defects behave as in the passive case with $x(t) \propto \sqrt{t_{\rm a} - t}$.

Building on these results, we now propose a phenomenological one-dimensional model that captures qualitatively the dynamics of pair annihilation in active nematics. Neglecting for simplicity the position dependence of the friction, which we assumed constant, the dynamics of a pair of disclinations initially at a distance x_0 along the x axis is governed by the equations:

$$\mu\,[\dot{x}_\pm - v_{\rm b}(x_\pm)] = \mp \frac{K}{x_+ - x_-} \tag{3}$$

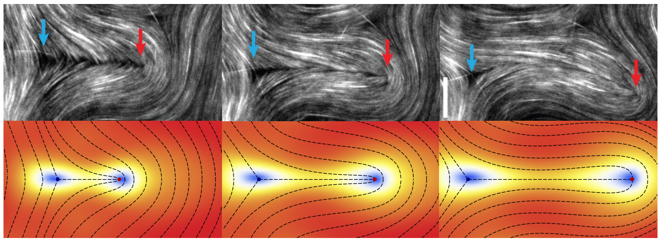

FIG. 2: Defect pair production in an active suspension of microtubules and kinesin (top) and the same phenomenon observed in our numerical simulation of an extensile nematic fluid with $\gamma = 100$ and $\alpha = -0.5$. The experimental picture is adapted by permission from Macmillan Publishers Ltd: Nature [16], copyright (2012).

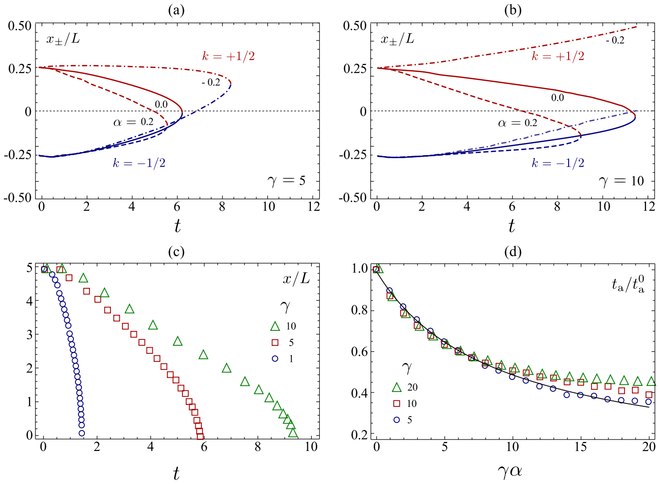

FIG. 3: Defect trajectories and annihilation times obtained from a numerical integration of Eqs. (1) for various γ and α values. (a) Defects trajectories for $\gamma = 5$ and various α values (indicated in the plot). The red and blue curve corresponds to the positive and negative disclination respectively. The defects annihilate where the two curves merge. (b) Same plot for $\gamma = 10$. Slowing down the relaxational dynamics of the nematic phase increases the annihilation time and for $\alpha = -0.2$ reverses the direction of motion of the $+1/2$ disclination. (c) Defect separation as a function of time for $\alpha = -0.2$ and various γ values. (d) Annihilation time normalized by the corresponding annihilation time obtained at $\alpha = 0$ (i.e. $t_{\rm a}^0$). The line is a fit to the model described in the text.

where $v_{\rm b}(x_\pm)$ is the backflow field at the position $x_\pm$ of the $\pm 1/2$ defect, given by $v_{\rm b}(x) = v_+(x - x_+) + v_-(x - x_-)$, with $v_\pm(x)$ the flow field due to an isolated $\pm 1/2$ defect. We retain only the active contribution to the the backflow and further simply replace the flow profiles by their constant values at the core of the defect, with $v_{\rm b}(x_+) = v_\alpha \propto \alpha$ and $v_{\rm b}(x_-) = 0$. Note that $v_\alpha > 0$ for contractile systems and $v_\alpha < 0$ for tensile ones. This yields the following simple equation for the pair separation:

$$\dot{x} = -v_\alpha - \frac{2\kappa}{x}\,, \tag{4}$$

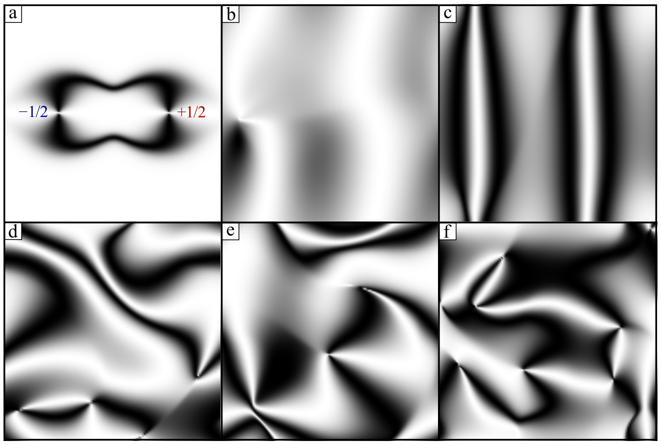

FIG. 4: Schlieren texture highlighting the post-collisional dynamics of a ±1/2 pair for $\gamma = 10^3$ and $\alpha = 0.2$. (a) Indicates the initial configuration of the defects and (b) shows the system immediately after defect annihilation.

where $\kappa = K/\gamma$. This equation manifestly captures the two regimes shown in Fig. 3c and described earlier. Eq. (4) can then be easily solved in the form:

$$x(t) = x_0 - v_\alpha t + 2(\kappa/v_\alpha)\ln\left[\frac{x(t) - 2\kappa/v_\alpha}{x_0 - 2\kappa/v_\alpha}\right] . \qquad (5)$$

The pair annihilation time t_a is defined by $x(t_a) = 0$ and is given by $t_a = x_0/v_\alpha - (2\kappa/v_\alpha^2)\ln[1 + (x_0 v_\alpha/2\kappa)]$. For $\alpha = 0$ this reduces to $t_a^0 = x_0^2/4\kappa$. In contractile systems activity speeds up pair annihilation while it slows it down in extensile systems. Our simple model predicts that the annihilation time normalized to its value in passive systems, t_a/t_a^0, depends only on $v_\alpha x_0/2\kappa \sim \alpha\gamma$. Fig. 3d shows a fit of the annihilations times extracted from the numerics to this simple formula. The model qualitatively captures the numerical behavior. As seen from the numerical solution of the full hydrodynamic equations, the trajectories of the two disclinations become asymmetric as α is increased, with the +1/2 defects speeding up towards the −1/2 defect. At large friction the attractive interaction in Eq. (3) becomes less and less important relative to the backflow, again consistent with the numerics.

While the effect of activity on the pre-collisional dynamics of a disclination pair can be accounted for relatively simply in terms of active backflow, the post-collisional behavior is dramatically affected by activity [27]. Recent experiments on tensile active suspensions of microtubule bundles crosslinked by kynesin clusters have shown activity have shown prominent examples of defects proliferation [16]. Fig. 4 shows the evolution of the system after annihilation of the initial defect pair. Fig. 4a frame shows the initial configuration of the two defects while 4b shows the configuration just after pair annihilation. The other frames display the evolution in time (with time increasing from left to right and top to bottom). Immediately after collision, the system develops two density/flow bands reminiscent of those observed in absence of defects [12]. The bands, however, are unstable and quickly start deforming while new defect pairs "pinch off". The dynamics quickly becomes chaotic, with frequent events of defect formation and annihilation on the background of an overall proliferation of defects. The passage of defects through a region of space lowers the local nematic order parameter in that region. Furthermore at large friction γ the slow relaxation prevents the restoration of the order parameter to its initial value, leading to a progressive reduction of the average order parameter in time. More work is needed to fully explore this rich and complex dynamics and formulate a quantitative classification of the behavior of defects in active liquid crystals.

We thank Zvonimir Dogic and Tim Sanchez for several illuminating discussions. LG was supported by SISSA mathLab. MCM was supported by the National Science Foundation through awards DMR-1004789 and DGE-1068780. MJB and X. Ma were supported by the National Science Foundation through award DMR-0808812 and by funds from the Soft Matter Program of Syracuse University.

[1] M. C. Marchetti, J. F. Joanny, S. R. Ramaswamy, T. B. Liverpool, J. Prost, M. Rao, and R. A. Simha, Rev. Mod. Phys. *to appear*, preprint arXiv:1207.2929 (2013).

[2] R. Voituriez, J. F. Joanny and J. Prost, Europhys. Lett. **70**, 118102 (2005).

[3] D. Marenduzzo, E. Orlandini, M. E. Cates, and J. M. Yeomans, Phys. Rev. E **76**, 031921 (2007).

[4] L. Giomi, M. C. Marchetti and T. B. Liverpool, Phys. Rev. Lett. **101**, 198101 (2008).

[5] S. Ramaswamy, R. A. Simha and J. Toner, Europhys. Lett. **62**, 196 (2003).

[6] S. Mishra and S. Ramaswamy, Phys. Rev. Lett. **97**, 090602 (2006).

[7] V. Narayan, S. Ramaswamy, and N. Menon, Science 317, **105** (2007).

[8] A. Sokolov and I. S. Aranson, Phys. Rev. Lett. **103**, 148101 (2009).

[9] L. Giomi, T. B. Liverpool and M. C. Marchetti, Phys. Rev. E **81**, 051908 (2010).

[10] S. M. Fielding, D. Marenduzzo and M. E. Cates, Phys. Rev. E **83**, 041910 (2011).

[11] L. Giomi, L. Mahadevan, B. Chakraborty and M. F. Hagan, Phys. Rev. Lett. **106**, 218101 (2011).

[12] L. Giomi, L. Mahadevan, B. Chakraborty and M. F. Hagan, Nonlinearity **25**, 2245 (2012).

[13] H. H. Wensink, J. Dunkel, S. Heidenreich, K. Drescher, R. E. Goldstein, H. Löwen and J. M. Yeomans, Proc. Natl. Acad. Sci. USA **109**, 14308 (2012).

[14] M. Kleman and O. Lavrentovich, *Order and Disorder in Soft Matter Physics* (Springer, 2002).

[15] R. Kemkemer, D. Kling, D. Kaufmann and H. H. Gruler, Eur. Phys. J. B **1**, 215-225 (2000).

[16] T. Sanchez, D. N. Chen, S. J. DeCamp, M. Heymann, and Z. Dogic, Nature **491**, 431 (2012).

[17] K. Kruse, F. Joanny, F. Jülicher, J. Prost, and K. Sekimoto, Phys. Rev. Lett. **92**, 078101 (2004).

[18] K. Kruse and F. J. Jülicher, Eur. Phys. J. E **20**, 459 (2006).

[19] R. Voituriez, J. F. Joanny, and J. Prost, Phys. Rev. Lett. **96**, 28102 (2006).

[20] J. Elgeti, M. E. Cates, and D. Marenduzzo, Soft Matter **7**, 3177 (2011).

[21] P. G. de Gennes and J. Prost, *The Physics of Liquid Crystals* (Clarendon Press, Oxford, Oxford, 1993).

[22] C. Denniston, Phys. Rev. B **54**, 6272 (1996).

[23] G. Tóth, C. Denniston, and J. M. Yeomans, Phys. Rev. Lett. **88**, 105504 (2002).

[24] E. I. Kats, V. V. Lebedev, and S. V. Malinin, J. Exp. Theor. Phys. **95**, 714 (2002).

[25] H. Pleiner, Phys. Rev. A **37**, 3986 (1988).

[26] G. Ryskin and M. Kremenetsky, Phys. Rev. Lett. **67**, 1574 (1991).

[27] S P. Thampi, R. Golestanian and J. M. Yeomans, preprint arXiv:1302.6732 (2013).